Molecular Therapy
Nucleic Acids
Original Article

Direct cardiac reprogramming via combined CRISPRa-mediated endogenous Gata4 activation and exogenous Mef2c and Tbx5 expression

Peisen Huang,[1,2,3] Jun Xu,[1,2,3] Benjamin Keepers,[1,2] Yifang Xie,[1,2] David Near,[1,2] Yangxi Xu,[1,2] James Rock Hua,[1] Brian Spurlock,[1,2] Shea Ricketts,[1,2] Jiandong Liu,[1,2] Li Wang,[1,2] and Li Qian[1,2]

[1]McAllister Heart Institute, University of North Carolina at Chapel Hill, Chapel Hill, NC 27599, USA; [2]Department of Pathology and Laboratory Medicine, University of North Carolina at Chapel Hill, Chapel Hill, NC 27599, USA

Direct cardiac reprogramming of fibroblasts into induced cardiomyocytes (iCMs) can be achieved by ectopic expression of cardiac transcription factors (TFs) via viral vectors. However, risks like genomic mutations, viral toxicity, and immune response limited its clinical application. Transactivation of endogenous TFs emerges as an alternative approach that may partially mitigate some of the risks. In this study, we utilized a modified CRISPRa/dCas9 strategy to transactivate endogenous reprogramming factors MEF2C, GATA4, and TBX5 (MGT) to induce iCMs from both mouse and human fibroblasts. We identified single-guide RNAs (sgRNAs) targeting promoters and enhancers of the TFs capable of activating various degrees of endogenous gene expression. CRISPRa-mediated *Gata4* activation, combined with exogenous expression of *Mef2c* and *Tbx5*, successfully converted fibroblasts into iCMs. Despite extensive sgRNA screening, transactivation of *Mef2c* and *Tbx5* via CRISPRa remained less effective, potentially due to *de novo* epigenetic barriers. While future work and refined technologies are needed to determine whether cardiac reprogramming could be achieved solely through CRISPRa activation of endogenous factors, our findings provide proof of concept that reliance on exogenous TFs for reprogramming can be reduced through CRISPRa-mediated activation of endogenous factors, particularly *Gata4*, offering a novel strategy to convert scar-forming fibroblasts into iCMs for regenerative purposes.

INTRODUCTION

Acute myocardial infarction (AMI) and subsequent heart failure have remained the leading cause of death worldwide for decades, placing a substantial burden on public health.[1] AMI can lead to the loss of nearly 25% of cardiomyocytes within just a few hours,[2] which triggers adverse cardiac fibrosis and ventricular remodeling. While effective revascularization therapies such as percutaneous coronary intervention, thrombolytic treatment, and coronary artery bypass grafting have been developed to restore blood flow to the myocardium,[3] they do not fully address the fundamental issues of cardiomyocyte loss. Although recent studies have shown that mammalian cardiomyocytes possess some regenerative capacity, the renewal rate is exceedingly slow and insufficient to compensate for the significant loss of cardiomyocytes following AMI.[4–7] Therefore, it is of great importance to explore new strategies to achieve myocardial repair and regeneration.

Direct reprogramming refers to the conversion of somatic cells into another type of mature somatic cell without passing through an intermediate multipotent progenitor or stem cell stage.[8] Since 2012, studies have demonstrated the use of viruses to directly reprogram fibroblasts into induced cardiomyocyte-like cells (iCMs) that are phenotypically and functionally similar to cardiomyocytes.[9–12] Forced expression of three cardiac transcription factors (TFs), *Mef2c*, *Gata4*, and *Tbx5* (MGT), has been shown to transform fibroblasts into functional cardiomyocytes *in vitro*.[9] By using the same TF cocktail in an *in vivo* mouse model of AMI, approximately 35% of cardiac fibroblasts (CFs) in the border/infarcted zone were successfully converted into iCMs, making a significant breakthrough in efforts to develop novel therapies based on *in vivo* lineage reprogramming.[10] As cardiac reprogramming rapidly advances toward translational application, there is a pressing need to develop reprogramming approaches that faithfully recapitulate cardiomyocyte phenotypes. Therefore, investigating whether and how endogenous activation of cardiac TFs can lead to iCMs is critical to the field.

CRISPR-Cas9 is a powerful, rapidly optimized gene-editing technology that has been adapted for a wide range of applications. By introducing mutations in both endonuclease domains, Cas9 can be engineered into an endonuclease dead form (dCas9) capable of delivering functional protein domains to genomic loci of interest.[13,14] When transcriptional

Received 11 March 2024; accepted 12 November 2024;
https://doi.org/10.1016/j.omtn.2024.102390.

[3]These authors contributed equally

Correspondence: Li Wang, McAllister Heart Institute, University of North Carolina at Chapel Hill, Chapel Hill, NC 27599, USA.
E-mail: liwang2020@whu.edu.cn
Correspondence: Li Qian, McAllister Heart Institute, University of North Carolina at Chapel Hill, Chapel Hill, NC 27599, USA.
E-mail: li_qian@med.unc.edu

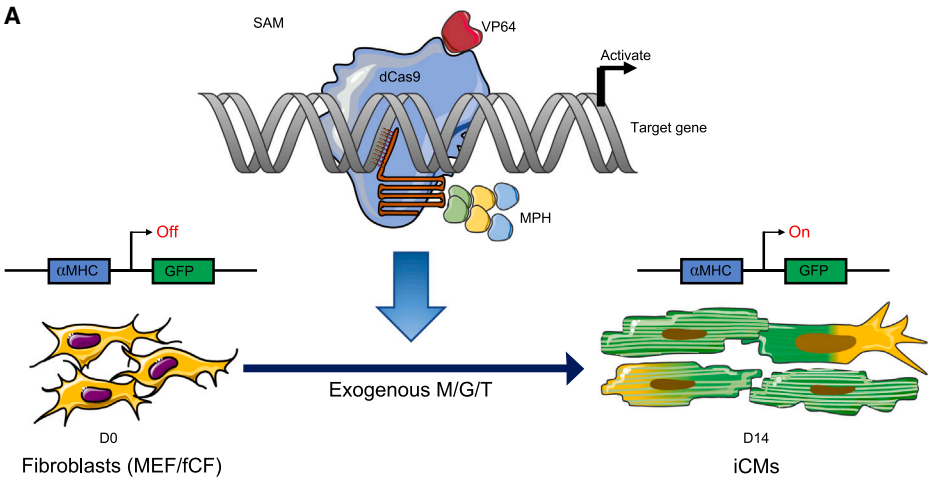

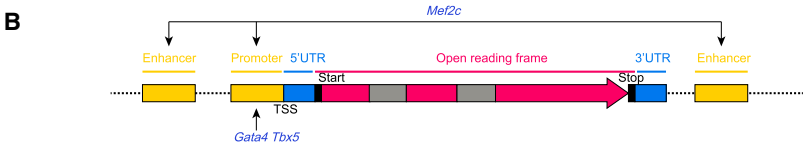

Steps to design sgRNAs targeting *Mef2c*/*Gata4*/*Tbx5*

1.Define TSS (transcription starting site)

-UCSC genome browse

2. Define promoter sequence

-*Gata4*

Annotates from Ensemble

-*Mef2c* & *Tbx5*:

Prediction

Empirical choice of sequence

Narrow range: -0.5 kb of TSS

Broad range: -2k to +2k of TSS

Enhancers: according to references

3. Design sgRNAs

-Benchling

-Sequence Scan for CRISPR

http://crispr.dfci.harvard.edu/SSC/

-CHOPCHOP

http://chopchop.rc.fas.harvard.edu/

4. Distal consideration

-Minimal 100bp distance between two neighbor sgRNAs

(legend on next page)

activators, such as VP64, are fused to the dCas9 protein, endogenous expression can be efficiently activated by targeting the dCas9 activator to the *cis*-acting elements of a target gene, a strategy known as CRISPR-based gene activation (CRISPRa).[15] Since CRISPRa-based strategies activate endogenous gene expression, they may offer a safer alternative for clinical applications than approaches relying on exogenous expression. Furthermore, the discovery of smaller Cas enzymes has simplified delivery methods, making it possible to package single-guide RNA (sgRNAs) and dCas9 protein into nanoparticles. This advancement holds great potential to mitigate the safety risk associated with viral-based delivery methods and facilitate the translation of direct cardiac reprogramming into clinical application.

In this study, we show that CRISPRa targeting both promoter regions close to the transcription start site (TSS) and enhancer regions distant from the TSS can activate endogenous expression of the cardiac reprogramming factors MGT. We then evaluated the capacity of endogenous MGT expression to reprogram mouse embryonic fibroblasts (MEFs), mouse fresh CFs (fCFs), and human H9-derived fibroblasts (H9F). By combining endogenous *Gata4* expression through CRISPRa with exogenous *Mef2c* and *Tbx5* expression from retroviruses, we successfully converted MEFs and H9F into iCMs. Additionally, we screened 124 sgRNAs for *Mef2c* and 18 sgRNAs for *Tbx5* with limited success in transactivating these two genes, likely due to the inaccessibility nature of the chromatin regions at the genomic loci. Nevertheless, the combinatorial approach of *Gata4* transactivation with exogenous overexpression of *Mef2c* and *Tbx5* to generate iCMs provides a proof of principle for future refinement of this strategy.

RESULTS

Experimental design

We utilized the second-generation CRISPRa system known as synergistic activation of mediators (SAM),[16] which consists of a dCas9-VP64 fusion, a sgRNA containing two MS2 RNA aptamers, and the MCP-p65-hsf1 (MPH) activation helper protein. Using this system to activate endogenous MGT expression, we aimed to leverage SAM CRISPRa to induce cardiac reprogramming (Figure 1A). To begin, we analyzed the structure of the MGT loci to locate their TSSs (narrow range: −0.5 kb of TSS; broad range: −2 kb to +2 kb of TSSs), their promoters, and potential upstream and downstream enhancers. We designed MGT-targeting sgRNAs for these regions using the algorithms Chopchop, Benchling, and Sequence Scan for CRISPR, excluding those with high off-target scores for testing (Figure 1B).

Initial tests of VP64 and SAM activators in MEFs

We began by comparing the performance of the first-generation dCas9-VP64 CRISPRa platform with the SAM system by evaluating their ability to activate endogenous *Gata4* in MEFs 3 days post-transfection (Figure 2A). The SAM system activated *Gata4* expression approximately 150-fold, whereas dCas9-VP64 alone achieved only a 5- to 10-fold activation (Figure 2B). Based on these results, we opted to use the SAM system for the remainder of the study.

Activation of endogenous *Gata4* in MEFs and fCFs with dCas9-SAM system

We designed an additional 15 candidate sgRNAs targeting the mouse *Gata4* gene (G-sgRNAs) between −1 kbp and +200 bp of the TSS. MEF and fCF were infected with lentiviruses encoding the SAM components and the sgRNAs, and *Gata4* transactivation was measured after antibiotic selection. The sequence, location, and activation efficiency of each sgRNA are detailed in Table S1. Compared to mock and non-targeted SAM control, activation of endogenous *Gata4* by G-sgRNAs was significantly increased in MEFs, with *Gata4*-sgRNAs 2, 3, 6, and 10 (G2, G3, G6, and G10) showing the highest activation. These four G-sgRNAs were located between −600 and 0 bp of TSS of *Gata4* (Figure 2C).

We then tested whether the co-expression of G2, G3, G6, and G10 in various combinations would further enhance *Gata4* transactivation. In MEF, G10 alone mediated the highest activation (284.69 ± 18.10-fold higher than endogenous *Gata4* expression), and combining two or three G-sgRNAs significantly boosted the expression level to a 500-fold increase (Figure 2D). In contrast, in fCFs, the activation of endogenous *Gata4* by G-sgRNAs was lower, with G10 mediating the highest degree of activation (approximately 3-fold), and combining multiple sgRNAs did not further enhance transactivation (Figure 2E).

To determine whether *Gata4* transactivation also leads to increased protein levels, we compared the effect of SAM CRISPRa with G-sgRNAs and the overexpression of *Gata4* using retrovirus (pMx-*Gata4*) by analyzing GATA4 protein levels at different time points post-infection. Both the pMx-*Gata4* and G-sgRNA groups significantly increased GATA4 protein levels in MEFs (Figure 2F). A time course analysis of protein expression revealed that exogenous GATA4 expressed by the pMx-*Gata4* retroviral vector peaked at day 3, while G-sgRNA-mediated activation of endogenous GATA4 reached a peak at day 5 (Figure 2G).

Activation of endogenous *Mef2c* in MEFs and fCFs with dCas9-SAM system

A total of 124 candidate *Mef2c* sgRNAs (M-sgRNAs) were designed targeting −2 to +2 kbp from the TSS and three enhancers of the *Mef2c* gene (Table S2). The three enhancers convey muscle, heart field, and endothelial cell-specific expression of *Mef2c*.[17–19] The results revealed that compared to the mock and non-targeted SAM

Figure 1. Graphical representation of cardiac reprogramming by CRISPR-dCas9-based transcriptional activators and sgRNAs design criteria

(A) Schematic of reprogramming mouse embryonic fibroblasts (MEFs) and fresh cardiac fibroblasts (fCFs) into induced cardiomyocytes (iCMs) via SAM system-mediated gene activation. Activation of transcriptional factors, including *Gata4*, *Mef2C*, and *Tbx5*, can reprogram MEFs and fCFs toward iCMs. (B) A graphical workflow for efficient sgRNA design. The process includes defining the TSS, retrieving the promoter sequence, designing sgRNAs, and considering distal regulatory elements for optimal sgRNA performance.

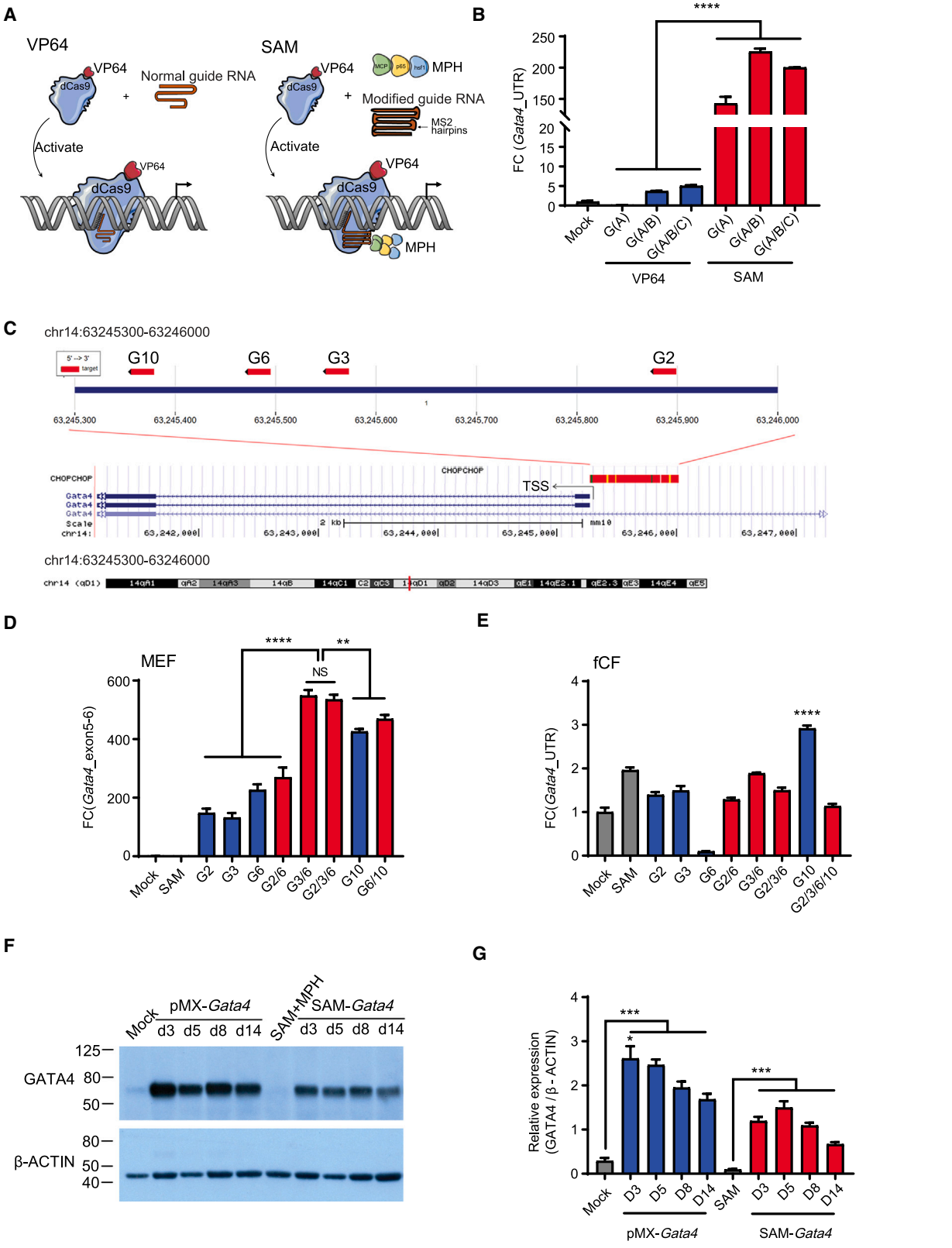

(legend on next page)

controls, most of the M-sgRNAs failed to effectively activate endogenous *Mef2c* expression (*Mef2c*_UTR) except for designed *Mef2c*-sgRNAs 25, 44, 94, 102, and 113 (M25, M44, M94, M102, and M113). We then tested the activation efficiency of these five sgRNAs individually and in combination. M94, M102, and M113, which are targeted to the heart field expression of *Mef2c*, mediated the highest level of transactivation in MEFs and fCFs (Figure 3A). In MEFs, a single M-sgRNA activated *Mef2c* expression to 1.60 ± 0.09-fold higher than endogenous *Mef2c*, and the combined use of two or three M-sgRNAs increased expression by around 6-fold (Figure 3B). In fCFs, a single M-sgRNA activated *Mef2c* 2.99 ± 0.06-fold. Multiple M-sgRNAs in combination did not further enhance transactivation (Figure 3C). Although the single M-sgRNA activated *Mef2c* at the mRNA level, SAM-*Mef2c* failed to activate MEF2C at the protein level in both CFs and MEFs (Figures 3D and 3E), suggesting the inefficacy of the sgRNA. Future work should focus on improving transactivation, not only for Mef2c but also for other reprogramming factors, by utilizing AI-based sgRNA efficiency prediction and leveraging new knowledge about novel enhancer and promoter regions.

Activation of endogenous *Tbx5* in MEFs and fCFs with dCas9-SAM system

We designed 18 candidate *Tbx5* sgRNAs (T-sgRNAs) targeting regions spanning −2 to +2 kbp from the TSS (Table S3). Most T-sgRNAs did not effectively activate endogenous *Tbx5* expression compared to the mock and non-targeted SAM controls. However, *Tbx5*-sgRNAs 5, 12, and 16 (T5, T12, and T16), located within the −600- to 0-kbp region of the *Tbx5* TSS, showed significant activation (Figure 4A). In MEFs, T16 alone activated *Tbx5* expression (*Tbx5*_UTR) approximately 34.74 ± 4.50-fold. Interestingly, unlike *Gata4* and *Mef2c* CRISPRa, combining multiple T-sgRNAs unexpectedly reduced transactivation compared to T16 alone (Figure 4B). In fCF, T16 and T5 each activated *Tbx5* by about 7-fold. No further increase in transactivation was observed with T-sgRNA combinations (Figure 4C). To determine whether *Tbx5* transactivation also led to increased protein levels, we compared the effect of SAM CRISPRa with T-sgRNAs to *Tbx5* overexpression using the pMx-*Tbx5* retrovirus at different time points post-infection. Compared with the mock and non-targeted SAM controls, pMx-*Tbx5* significantly increased the expression of TBX5 protein level in MEFs. At the same time, the T-sgRNA group only showed a modest increase in TBX5 protein expression, which did not reach statistical significance (Figures 4D and 4E).

OCT1 does not boost sgRNA expression

OCT1 is a widely expressed protein in mammalian cells that recognizes a conserved octamer sequence.[20] Previous studies have reported that *Oct1* overexpression enhances sgRNA expression by increasing U6 promoter activity.[21] To test whether *Oct1* can augment the expression of MGT sgRNAs, we used a lentiviral-based system to overexpress *Oct1*. Although successful overexpression of *Oct1* was confirmed (Figure S1A), no enhancement of CRISPRa activity for MGT sgRNAs was observed (Figures S1B–S1G). Thus, *Oct1* overexpression was not used in subsequent experiments.

CRISPRa-mediated activation of *Gata4* in combination with ectopic retroviral *Mef2c* and *Tbx5* expression induces cardiac reprogramming in MEF

Since the G-sgRNAs demonstrated the highest efficiency in activating their target genes, we evaluated whether CRISPRa-mediated *Gata4* expression, in combination with ectopic retroviral expression of *Mef2c* and *Tbx5*, could improve reprogramming efficiency compared to pMx-MT or pMx-MGT (Figure 5A). Flow cytometry analysis revealed significant induction of α-major histocompatibility complex (αMHC)-GFP and cardiac troponin T (cTnT) by pMx-MT+SAM, pMx-MT+SAM-*Gata4*, and pMx-MGT, with the highest efficiency observed in the pMx-MT+SAM-*Gata4* group (12.77% αMHC-GFP$^+$ and 3.03% cTnT$^+$; Figures 5B and 5C). Additionally, quantitative real-time PCR (real-time qPCR) was used to measure endogenous and total reprogramming factor expression levels, as well as cardiomyocyte and fibroblast markers, on 8 days post-infection (Figure 5D). Endogenous *Gata4* expression was effectively activated by SAM-*Gata4*, while total *Gata4* expression (*Gata4*_Exo5/6) was the highest in the pMGT group, indicating specific activation of *Gata4* by CRISPRa, albeit to a lesser extent than ectopic retroviral *Gata4* expression. The expression of sarcomere components and myosin-related genes (*Actc1*, *Tnnt2*, *Myh6*, *Myl4*, *Myl7*) was increased in both the pMx-MT+SAM-*Gata4* and pMx-MGT groups compared to pMx-MT+SAM. Similarly, the expression of *Pln* and *Slc8a1*, which encode key regulators of calcium handling in cardiomyocytes, was highest in the pMx-MT+SAM-*Gata4* and pMx-MGT groups. In contrast, fibroblast gene expression (*Postn*, *Col1a1*, *Col1a2*, *Tcf21*) significantly decreased in all three reprogrammed groups compared to the mock group. Immunofluorescence staining for αMHC-GFP and cTnT confirmed successful cardiac reprogramming in the pMT+SAM-*Gata4* and pMx-MGT groups (Figures 4E and 4F). In conclusion, the dCas9-G-sgRNA-mediated activation of endogenous *Gata4*, when combined with ectopic pMx-MT, can substitute for retroviral *Gata4* overexpression to improve the direct cardiac reprogramming of MEFs.

CRISPRa-mediated activation of endogenous MGT promotes certain cardiac gene expression and suppresses the fibroblast gene program in MEFs and fCFs

After successfully replacing ectopic *Gata4* expression with SAM-*Gata4* in MEF reprogramming, we investigated whether

Figure 2. Evaluation of VP64 and SAM systems for *Gata4* activation in MEFs in MEFs and fCFs

(A) Schematic of the different systems tested. (B) Comparative analysis of the VP64 and SAM system for *Gata4* activation in MEFs. (C) Schematic showing the location of the efficient sgRNA-targeted sites for *Gata4* with all four efficient *Gata4*-sgRNAs (G-sgRNAs) located in −600 to 0 kb of the TSS for the *Gata4* gene. (D and E) Transcriptional activation of endogenous *Gata4* (*Gata4*_UTR) in MEFs (D) and fCFs (E) using the SAM system. (F and G) Western blotting analysis of GATA4 protein levels in MEFs with targeted activation (SAM-*Gata4*) or ectopic overexpression (pMx-*Gata4*) of *Gata4* at various time points post-infection. *$p < 0.05$; **$p < 0.01$; ***$p < 0.001$; ****$p < 0.0001$.

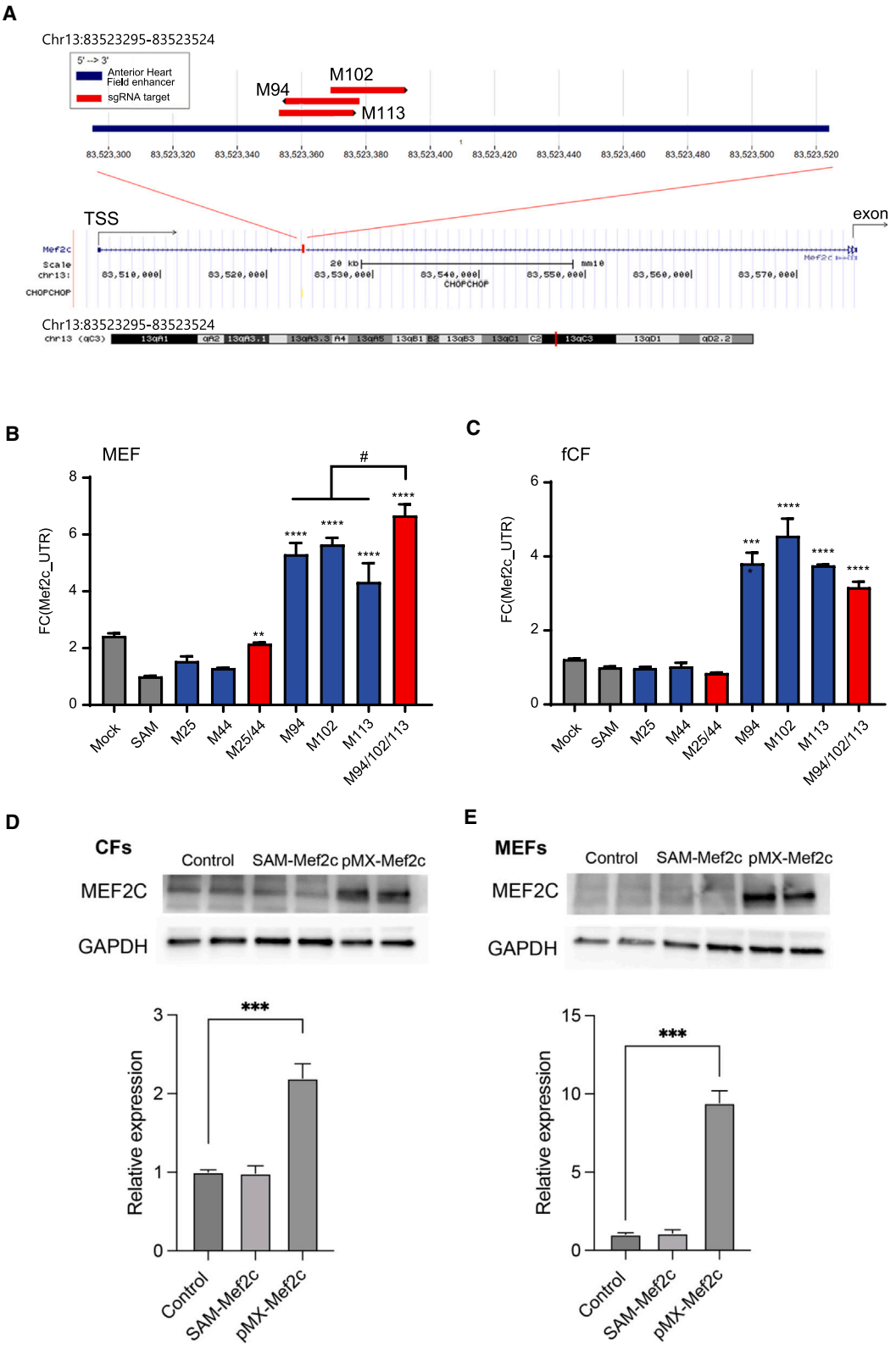

(legend on next page)

activating all three reprogramming factors using CRISPRa could induce cardiac reprogramming. Using the best-performing M-sgRNA, G-sgRNA, and T-sgRNA from our screening in MEF, we tested whether SAM-mediated activation of *Mef2c*, *Gata4*, and *Tbx5* (SAM-MGT) could reprogram both MEFs and fCFs. In MEFs, the proportion of αMHC-GFP$^+$ cells in the SAM-MGT group was significantly higher than that in the mock group (1.86 ± 0.58% vs. 0.31 ± 0.03%, $p = 0.02$) and the non-targeted SAM group (1.86 ± 0.58% vs. 0.55 ± 0.19%, $p = 0.04$). However, the proportion of cTnT$^+$ cells did not increase compared to the non-targeted SAM group (Figures S2A and S2B). While SAM-MGT increased both endogenous and total expression of *Gata4* and *Tbx5*, it did not induce *Mef2c* expression. SAM-MGT also upregulated the expression of some cardiac genes, like *Actc1*, *Tnnt2,* and *Slc8a1*, while downregulating fibroblast markers (Figure S2C). Moreover, immunofluorescence staining showed that a small number of GFP$^+$/cTnT$^+$ cells could be found (Figure S2D). These results demonstrate that CRISPRa-mediated activation of endogenous *Gata4* and *Tbx5* without activation of *Mef2c* enhances certain cardiac gene expression and suppresses fibroblast gene program in MEFs, although this effect appears to yield minimal or negligible cardiac reprogramming.

For fCF reprogramming, flow cytometry analysis showed a marginally higher ratio of GFP$^+$ and cTnT$^+$ cells than the mock group. However, this increase was not statistically significant compared to the non-targeted SAM group (Figures S2E and S2F). In contrast to the results observed in MEFs, fCF reprogramming resulted in a substantial increase in the expression of cardiomyocyte structural and ion channel markers in the SAM-MGT group relative to the mock group (Figure S2G). Nevertheless, the overall proportion of GFP$^+$ and cTnT$^+$ cell ratio remained low, as indicated by immunofluorescence staining (Figure S2H). The data suggest that inherent differences in the starting fibroblast populations may result in significantly different reprogramming outcomes independent of the reprogramming approaches employed.

Human cardiac reprogramming using CRISPRa

Next, we initiated the reprogramming of human fibroblasts into iCMs by designing and testing sgRNAs, focusing primarily on potential target sites near the TSS, as proximity to the TSS is strongly associated with sgRNA-mediated gene activation.[22] For this purpose, we targeted the TSS of NCBI RefSeq transcripts for each reprogramming factor, as well as those from transcripts with high expression in human ventricular tissue, according to data from the GTEx database.[23] In addition to the TSS regions, we sought to identify potential sgRNA target sites with the cardiac-specific enhancers of the reprogramming factors, as cataloged in the VISTA database, which are known to be active during embryogenesis.[24] Finally, H3K27Ac enrichments at the MGT loci, as identified in the human cell lines from the ENCODE project, were considered to further optimize our selection of sgRNA target sites.[25]

We carried out multiple rounds of human sgRNA design, cloning into lentiSAMv2, and testing (Table 1). In each experiment, H9Fs were co-infected with the lentiSAMv2 clone and lentiMPHv2 followed by antibiotic selection and qPCR analysis. We found that the extent of CRISPRa-mediated gene activation varied significantly across sgRNAs and did not consistently correlate with their proximity to the TSS (Figures 6A–6C). Furthermore, siRNAs targeting the same genomic region exhibited considerable variability in gene activation, likely due to the intrinsic biochemical properties of the sgRNAs themselves rather than the targeted genomic regions.[26] Through these efforts, we identified two sgRNAs that resulted in a 50- to 70-fold activation of *MEF2C* compared to the non-targeted control (Figure 6A), while three sgRNAs achieved a 200- to 300-fold activation of *GATA4* (Figure 6B). Additionally, 11 sgRNAs were found to induce a 100- to 10,000-fold activation of *TBX5* (Figure 6C). These screening results indicate that CRISPRa-mediated activation of human MGT is achievable and represents a promising approach for inducing cardiac reprogramming.

Utilizing the most efficient sgRNA for each gene, we next sought to reprogram fibroblasts into human iCMs with the CRISPRa system. H9Fs were induced to overexpress *GATA4* with the CRISPRa system, while *MEF2C* and *TBX5* were overexpressed through retroviral delivery of their respective coding sequences (cDNAs), and *miR-133a2* was delivered as a precursor miRNA. The inclusion of miR-133a2 with MGT was based on previous reports indicating that *miR133a2* enhances the efficiency of human fibroblast conversion to iCMs.[27] To control for the potential effects that miR-133-a2 would have on MGT expression, miR-133a2 was included in all human reprogramming conditions in this study.

We first assessed the expression of *MGT* following CRISPRa-mediated activation of *GATA4*. No significant differences in *MEF2C* or *TBX5* expression were observed between non-targeting control (pMT–133+SAM), CRISPRa-mediated *GATA4* (pMT–133+SAM-*GATA4*), and retroviral *GATA4* (pMGT–133) groups, suggesting that CRISPRa-mediated activation of *GATA4* does not induce the expression of *MEF2C* or *TBX5*. However, CRISPRa-mediated *GATA4* expression was approximately 80-fold higher than in the non-targeting control, although still significantly lower than that achieved with retroviral *GATA4* expression (Figure 6D).

Ten days after initiating reprogramming, the samples with GATA4 CRISPRa exhibited a 14-fold change increase in MYH6 expression compared to both the negative control and retroviral-mediated reprogramming (Figure 6E). Although *TNNT2* expression was increased, the

Figure 3. Transcriptional activation of *Mef2c* in MEFs and fCFs using the SAM system

(A) Schematic of the sgRNA-targeted site for *Mef2c*, with all three efficient *Mef2c*-sgRNAs (M-sgRNAs) located within the anterior heart field enhancer of *Mef2c* gene. (B and C) Transcriptional activation of endogenous *Mef2c* (*Mef2c*_UTR) in MEFs (B) and fCFs (C) using the SAM activators. (D and E) Western blotting analysis of MEF2C protein levels in CFs (D) and MEFs (E) with targeted activation (SAM-Mef2c) or ectopic overexpression (pMx-Mef2c). $^{**}p < 0.01$; $^{****}p < 0.0001$.

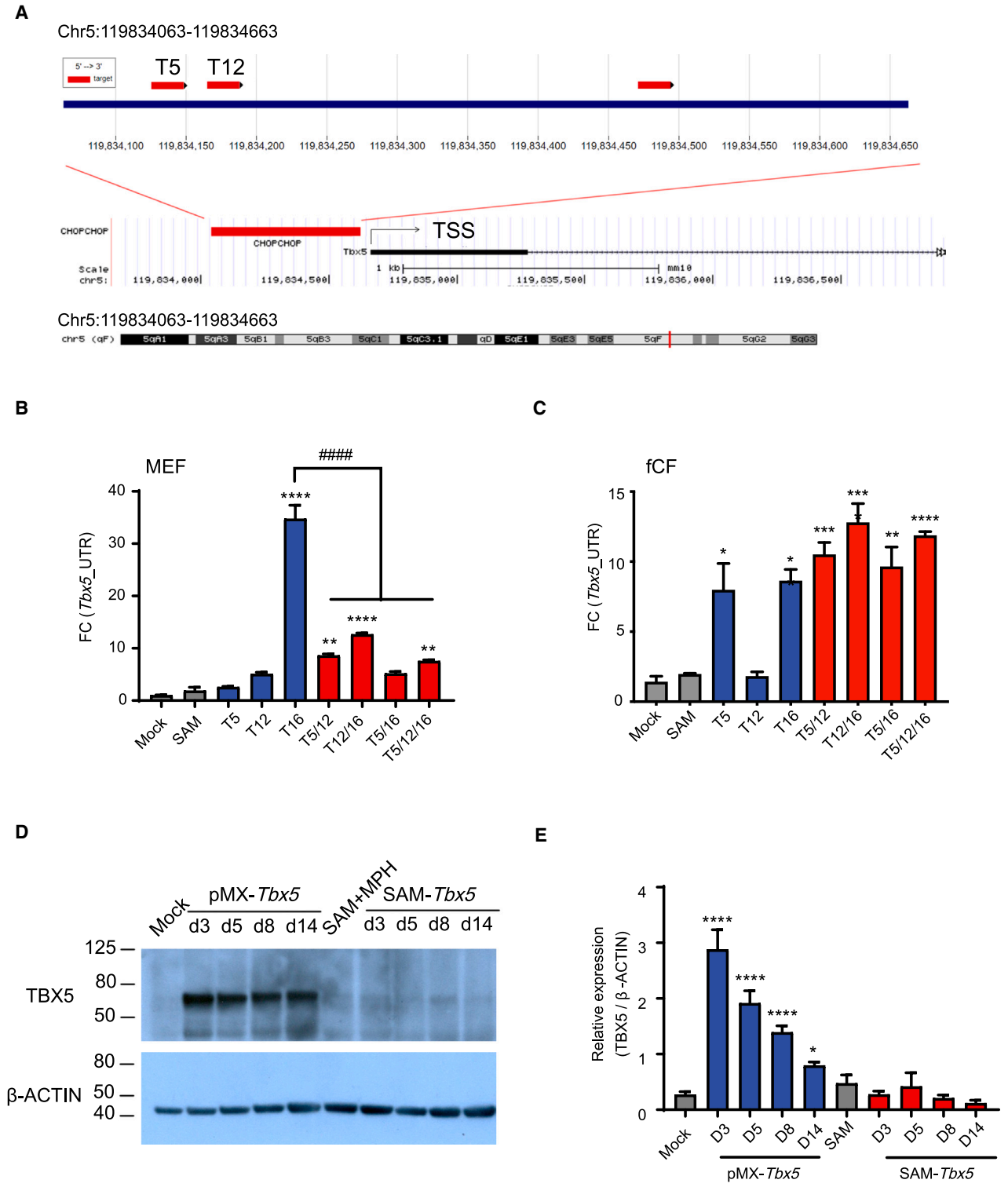

Figure 4. Transcriptional activation of *Tbx5* in MEFs and fCFs using the SAM system

(A) Schematic of sgRNA-targeted sites for *Tbx5* with all three efficient Tbx5-sgRNAs (T-sgRNAs) located in −600 to 0 kb of the TSS for the *Tbx5* gene. (B and C) Transcriptional activation of endogenous *Tbx5* (*Tbx5*_UTR) in MEFs (B) and fCFs (C) using the SAM system. (D and E) Western blotting analysis of TBX5 protein expression in MEFs following targeted activation (SAM-Tbx5) or ectopic overexpression (pMx-Tbx5) at various time points post-infection. *$p < 0.05$; **$p < 0.01$; ***$p < 0.001$; ****$p < 0.0001$.

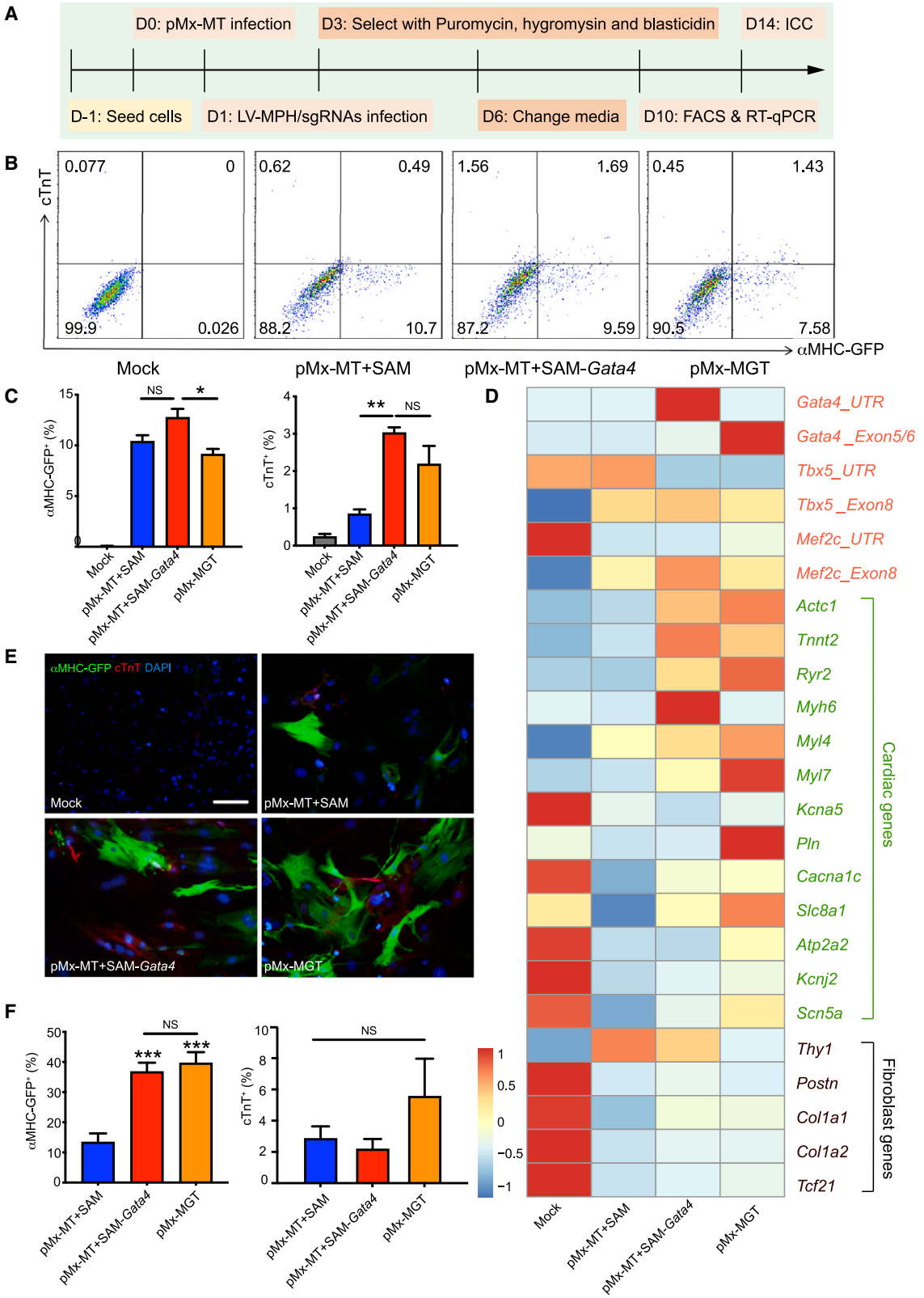

(legend on next page)

increase was not statistically significant compared to the control, and *ACTN2* expression levels were similar across samples. By day 14, human iCMs were observed in the sample with *GATA4* CRISPRa, as determined by immunofluorescence for cTnT, while no iCMs were detected in the negative control (Figure 6F). Together, these results suggest that CRISPRa-mediated activation of *GATA4* substantially contributes to human cardiac reprogramming.

We next attempted to reprogram human fibroblasts into iCMs by CRISPRa-mediated activation of all three MGT factors. H9Fs were infected with separate virus vectors, each encoding a sgRNA targeting *MEF2C*, *GATA4*, or *TBX5* in the human SAM-MGT system. By day 14, CRISPRa-induced activation reached approximately 70-fold for *MEF2C*, 1,000-fold for *TBX5*, and 4,000-fold for *GATA4*. When compared to retroviral MGT overexpression, CRISPRa-mediated activation of *TBX5* and *GATA4* was significantly lower, whereas no significant difference was observed for *MEF2C* expression (Figure 6G). Cardiomyocyte markers *TNNT2*, *NPPB*, and *SCN5A* were significantly upregulated in the CRISPRa-treated samples compared to the negative control (p133+SAM) (Figure 6G). Immunofluorescence staining for cTnT and α-actinin identified a limited number of human iCMs in the CRISPRa samples, although at a low frequency (Figure 6H). Notably, the cTnT signal in the CRISPRa-treated samples was qualitatively weaker, and the morphology of the human iCMs in these samples differed from those produced through retroviral MGT reprogramming. Taken together, these data indicate that a cardiac program in human fibroblasts can be activated by CRISPRa of MGT.

DISCUSSION

In this study, we reprogrammed fibroblasts to iCMs through targeted activation of endogenous reprogramming factors. We utilized the second-generation SAM CRISPRa system as a programmable and transcriptional regulator to activate the expression level of *Mef2c*, *Gata4*, and *Tbx5* in both mouse and human fibroblasts. Our findings demonstrate that endogenous activation of *Gata4* via CRISPRa could effectively substitute for ectopic retroviral *Gata4* expression in the reprogramming process.

A comparative study of second-generation CRISPRa platforms, including VPR, SAM, and SunTag, identified SAM as the most effective system.[15] In our study, we corroborated this finding, demonstrating that SAM was more effective than the first-generation CRISPRa platform dCAS9-VP64. Notably, sgRNAs targeting *Gata4* achieved potent activation in MEFs, and the use of multiplex sgRNAs further enhanced activation. This result aligns with the study of Chavez et al., which showed that the combined use of multiple sgRNAs can synergistically promote target gene expression.[15,28] However, in MEFs, combining multiple T-sgRNAs produced a significant antagonistic effect on the transcriptional output compared to singlet T-sgRNAs (Figure 4B). This suggests that while the use of multiple sgRNA may theoretically enhance gene activation, empirical validation is necessary in each specific context. Additionally, we observed that the degree of gene activation varied between cell types, even when using the same sgRNA or sgRNA combination. In MEFs, for instance, several G-sgRNAs activated *Gata4* hundreds of times above the endogenous level, whereas in fCFs, the activation was less than 10-fold (Figures 2D and 2E). One potential explanation for this difference is the higher basal *Gata4* expression in fCFs compared to MEFs (Figure S3), indicating that CRISPRa-mediated gene activation may be inversely correlated with the basal expression level of the targeted gene, as previously described.[29]

Various strategies have been proposed for cardiac regeneration and repair, including cytokine administration, skeletal muscle myoblast transplantation, stem cell therapies, and engineered myocardial tissue patches.[30] While these approaches have shown promise in animal models, their clinical translation has yielded unsatisfactory outcomes.[31] A primary reason for these failures is likely the inability to fully address the permanent loss of cardiomyocytes and reverse the progressive decline in cardiac function. Direct cardiac reprogramming represents a promising alternative for repairing injured hearts.[9–11,32] However, traditional reprogramming methods, which rely on retroviral infection, pose significant challenges for clinical translation in myocardial regeneration.[32]

Several alternative approaches have been developed to replace retroviruses-based direct cardiac reprogramming. Mathison et al. constructed a proliferation-deficient-adenoviral GMT expression vector (Ad-GMT) and successfully achieved cardiac reprogramming both *in vitro* and *in vivo*.[33] Jayawardena et al. identified microRNA (miRNA) combinations, including miRNA-1, -133, -208, and -499, capable of inducing fibroblasts into iCMs.[34–36] Inspired by the use of small molecules for the generation of induced pluripotent stem cells, Fu et al. developed a small-molecule cocktail CRFVPTZ (C, CHIR99021; R, RepSox; F, Forskolin; V, VPA; P, Parnate; and T, TTNPB) that efficiently reprogrammed MEFs to iCMs.[37] These novel strategies represent significant progress toward the clinical translation of direct cardiac reprogramming. Our study provides evidence that cardiac reprogramming could be achieved with CRISPRa, presenting a theoretical opportunity to formulate nanoparticles loaded with SAM-MGT ribonucleoproteins for direct delivery to the border zone of an AMI, thereby circumventing the risks associated with using mutagenic retroviral vectors. The development of

Figure 5. Reprogramming MEFs into iCMs via SAM-mediated endogenous *Gata4* activation and pMx-MT-mediated *Mef2c* and *Tbx5* ectopic overexpression

(A) Schematic of reprogramming MEFs into iCMs using SAM-*Gata4* activation and pMx-MT overexpression. D, day; FACS, fluorescence-activated cell sorter; ICC, immunofluorescence staining. (B and C) Flow cytometry analysis of GFP^+ and $cTnT^+$ cells (B), with the corresponding statistical graphs (C) showing the percentage of GFP^+ or $cTnT^+$ cells in (B). (D) Heatmap displaying the expression levels of transcription factors and cardiac and fibroblast-related marker genes assessed by real-time qPCR on 10 days post-infection in the pMx-MT, pMx-MT+SAM-Gata4, pMx-MGT, and mock groups. (E and F) Immunofluorescence staining of GFP and cTnT on day 14 of reprogramming (E), with the corresponding statistical graph of the percentage of GFP^+ or $cTnT^+$ cells (F). Scale bar in (E), 100 μm. $^*p < 0.05$; $^{**}p < 0.01$; $^{****}p < 0.0001$.

Table 1. Results of human sgRNA testing

Gene	sgRNA ID	Target sequence	Experiment 1–replicate 1	Experiment 2–replicate 1	Experiment 2–replicate 2	Experiment 3–replicate 1	Experiment 3–replicate 2	Experiment 4–replicate 1	Experiment 4–replicate 2	Experiment 5–replicate 1	Experiment 5–replicate 2	Average vs. GAPDH	SEM
GATA4	sgGv1-A	GCCCAGCGGAGG TGTAGCCG	261.083	69.807	43.950	–	–	234.804	111.798	701.449	544.367	281.037	94.880
GATA4	sgGv1-B	TAGCACTTGGGC ATTTTCCG	21.432	–	–	–	–	–	–	–	–	21.432	NA
GATA4	sgGv1-C	CCTGTGGGAGTC ACGTGCAA	5.110	–	–	–	–	–	–	–	–	5.110	NA
GATA4	sgGv3-1	AGGGACCATGTA TCAGAGCTTGG	–	–	–	–	–	–	–	314.788	174.231	244.510	70.279
GATA4	sgGv3-2	TTGACCTGCGAG GGAGAGAGAGG	–	–	–	–	–	–	–	10.909	12.211	11.560	0.651
GATA4	sgGv3-4	GCGTGGCTCCTT GACCTGCGAGG	–	–	–	–	–	–	–	21.198	16.129	18.664	2.534
GATA4	sgGv3-5	TCGCAGGTCAAG GAGCCACGCGG	–	–	–	–	–	–	–	24.016	107.836	65.926	41.910
GATA4	sgGv3-6	CGCAGGTCAAGG AGCCACGCGGG	–	–	–	–	–	–	–	173.596	202.758	188.177	14.581
GATA4	sgGv4-1	TGAGGACTGAGT GCCGCGCAGGG	–	–	–	–	–	–	–	34.227	23.207	28.717	5.510
GATA4	sgGv4-2	GGCGGGCGGCG CAAACTCGGCGG	–	–	–	–	–	–	–	1.433	0.778	1.105	0.328
GATA4	sgGv4-3	CAGTACTTAAGG CACATCTAAGG	–	–	–	–	–	–	–	0.484	0.527	0.505	0.021
GATA4	sgGv4-4	AGAGAGGCAGAT GTATAGACAGG	–	–	–	–	–	–	–	0.747	0.930	0.839	0.092
GATA4	sgGv4-5	ATAAACGGGCCA AAGGTACCTGG	–	–	–	–	–	–	–	0.664	0.522	0.593	0.071
GATA4	sgGv4-6	ATCTTCAGTCATC AAGGATGGGG	–	–	–	–	–	–	–	0.793	0.757	0.775	0.018
GATA4	sgGv4-7	ATGTGATGCCCAG AGTCAGTGGG	–	–	–	–	–	–	–	0.581	0.836	0.708	0.128
GATA4	sgGv4-8	CTTCCTACGATGT TTATGACTGG	–	–	–	–	–	–	–	0.495	0.562	0.528	0.034
GATA4	sgGv4-9	AATTAAATACATC TACTGAGAGG	–	–	–	–	–	–	–	0.612	0.495	0.553	0.058
GATA4	sgGv4-10	TCAGCATTTATCC GGAGCGGGGG	–	–	–	–	–	–	–	0.758	0.911	0.835	0.077
MEF2C	sgMv1-A	TATCAAGGAAAT AAACTATA	1.133	–	–	–	–	–	–	–	–	1.133	NA
MEF2C	sgMv1-B	ATATATGGTATA TCACAGAC	0.873	–	–	–	–	–	–	–	–	0.873	NA

(*Continued on next page*)

Table 1. ***Continued***

Gene	sgRNA ID	Target sequence	Experiment 1–replicate 1	Experiment 2–replicate 1	Experiment 2–replicate 2	Experiment 3–replicate 1	Experiment 3–replicate 2	Experiment 4–replicate 1	Experiment 4–replicate 2	Experiment 5–replicate 1	Experiment 5–replicate 2	Average vs. GAPDH	SEM
MEF2C	sgMv1-R1A	TCAAGGAGGTAC AAAAGGAA	0.872	–	–	–	–	–	–	–	–	0.872	NA
MEF2C	sgMv1-R3A	GATGAAATGAAA AACTGGAG	1.592	–	–	–	–	–	–	–	–	1.592	NA
MEF2C	sgMv1-R2A	TCGTGCCAAGGA AAATGGAG	0.912	–	–	–	–	–	–	–	–	0.912	NA
MEF2C	sgMv1-R2B	AAAGTACAGTGG GCTAACAG	0.694	–	–	–	–	–	–	–	–	0.694	NA
MEF2C	sgMv2-9	CCTCCTCCTCCTC TTCCGAG	–	–	–	11.601	16.600	–	–	–	–	14.101	2.500
MEF2C	sgMv2-10	CCGAGGCCGCTC GGAAGAGG	–	–	–	57.353	62.174	96.684	98.050	44.579	53.283	68.687	9.373
MEF2C	sgMv2-15	CCTCGGCGCGCG CGAATGCG	–	–	–	0.734	0.959	–	–	–	–	0.847	0.112
MEF2C	sgMv2-17	CCGCGCATTCGC GCGCGCCG	–	–	–	0.672	0.708	–	–	–	–	0.690	0.018
MEF2C	sgMv3-1	AGCTGTGCAAGTG CTGAAGAAGG	–	–	–	–	–	43.275	64.776	–	–	54.026	10.750
MEF2C	sgMv3-3	ATATATGGTATATC ACAGACAGG	–	–	–	–	–	2.427	2.701	–	–	2.564	0.137
MEF2C	sgMv3-4	GTACCTGTGTATG CTAAGTAGGG	–	–	–	–	–	2.849	2.696	–	–	2.772	0.077
MEF2C	sgMv3-6	GCAGCTAATTCA TTTCTGAAGGG	–	–	–	–	–	1.633	1.735	–	–	1.684	0.051
MEF2C	sgMv3-8	CCATCCTATTTG CATAACGAGGG	–	–	–	–	–	1.155	1.421	–	–	1.288	0.133
MEF2C	sgMv3-9	CCCTCGTTATGC AAATAGGATGG	–	–	–	–	–	1.862	2.055	–	–	1.958	0.097
MEF2C	sgMv3-10	TCCATCCTATTT GCATAACGAGG	–	–	–	–	–	1.735	2.119	–	–	1.927	0.192
MEF2C	sgMv3-11	ACAGACATATCA TGTCTTTGTGG	–	–	–	–	–	2.609	3.066	–	–	2.837	0.229
MEF2C	sgMv3-12	ATTACATACTGG AGATCTCTGGG	–	–	–	–	–	2.058	2.641	–	–	2.350	0.291
MEF2C	sgMv3-13	ATACTGGAGATC TCTGGGTCAGG	–	–	–	–	–	4.082	3.801	–	–	3.941	0.140
MEF2C	sgMv3-14	GAAGAAAAACGG GGACTATGGGG	–	–	–	–	–	1.167	1.719	–	–	1.443	0.276
MEF2C	sgMv4-1	CTGGTCTGGCTT TATTCTGCAGG	–	–	–	–	–	–	–	0.859	0.786	0.823	0.037

(*Continued on next page*)

Table 1. ***Continued***

Gene	sgRNA ID	Target sequence	Experiment 1–replicate 1	Experiment 2–replicate 1	Experiment 2–replicate 2	Experiment 3–replicate 1	Experiment 3–replicate 2	Experiment 4–replicate 1	Experiment 4–replicate 2	Experiment 5–replicate 1	Experiment 5–replicate 2	Average vs. GAPDH	SEM
MEF2C	sgMv4-2	TGCCATTTTACA TGTTCCAGTGG	–	–	–	–	–	–	–	1.075	0.841	0.958	0.117
MEF2C	sgMv4-3	CACTTATTCAGTA CTCAGCTAGG	–	–	–	–	–	–	–	1.424	1.281	1.353	0.071
MEF2C	sgMv4-4	GGTTTATTGGTAA ACATGTATGG	–	–	–	–	–	–	–	1.155	1.144	1.150	0.005
MEF2C	sgMv4-5	ATATTACTTTTCA TCGAGGGTGG	–	–	–	–	–	–	–	0.904	0.852	0.878	0.026
MEF2C	sgMv4-6	CTACCAAACTCCA CTTTCAGTGG	–	–	–	–	–	–	–	1.116	1.354	1.235	0.119
MEF2C	sgMv4-7	CCAGAGCTAGGT TGTTTATGTGG	–	–	–	–	–	–	–	1.067	1.229	1.148	0.081
MEF2C	sgMv4-8	ATGGTGTGGTCT CACCTTACTGG	–	–	–	–	–	–	–	0.940	0.962	0.951	0.011
MEF2C	sgMv4-9	CTTGTCCAAGGT TCTGCCAAAGG	–	–	–	–	–	–	–	1.140	1.408	1.274	0.134
MEF2C	sgMv4-10	GACAAATACATA CTAATTTGAGG	–	–	–	–	–	–	–	1.041	1.036	1.038	0.003
TBX5	sgTv1-A	CAAATCATTTCA AACGCGGT	13.794	–	–	–	–	–	–	–	–	13.794	NA
TBX5	sgTv1-B	CTGCTTCTCTGA GCAAGCGG	20.402	–	–	–	–	–	–	–	–	20.402	NA
TBX5	sgTv1-C	TGAGTGTTCGG GAAATCTAG	10.990	–	–	–	–	–	–	–	–	10.990	NA
TBX5	sgTv2-12	GACGTCACGAG TCACGCAAC	–	–	–	0.122	0.086	–	–	–	–	0.104	0.018
TBX5	sgTv2-15	GCGCTGTCACG TTTGGCTGG	–	0.511	2.218	0.309	0.485	–	–	–	–	0.881	0.448
TBX5	sgTv2-34	GCCGCTGCACC TATAGGACT	–	–	–	0.141	0.113	–	–	–	–	0.127	0.014
TBX5	sgTv2-35	AAACGTGACAG CGCGCGGGC	–	–	–	0.751	0.594	–	–	–	–	0.673	0.079
TBX5	sgTv3-1	CACCATGGCCG ACGCAGACGAGG	–	–	–	–	–	6,851.464	4,704.819	–	–	5,778.141	1,073.323
TBX5	sgTv3-2	CTCAGAGCAGA ACCTTGCGCGGG	–	–	–	–	–	10,238.454	9,834.440	–	–	10,036.447	202.007
TBX5	sgTv3-4	CCTCAGAGCAG AACCTTGCGCGG	–	–	–	–	–	13,035.915	12,940.372	16.275	15.789	6,502.088	3,744.777
TBX5	sgTv3-5	TGCTCTGAGGAC AAGAAGCAGGG	–	–	–	–	–	1,843.998	1,637.516	–	–	1,740.757	103.241

(*Continued on next page*)

Table 1. ***Continued***

Gene	sgRNA ID	Target sequence	Experiment 1–replicate 1	Experiment 2–replicate 1	Experiment 2–replicate 2	Experiment 3–replicate 1	Experiment 3–replicate 2	Experiment 4–replicate 1	Experiment 4–replicate 2	Experiment 5–replicate 1	Experiment 5–replicate 2	Average vs. GAPDH	SEM
TBX5	sgTv3-8	GCACAATTCTAGT GACAGGAGGG	–	–	–	–	–	30,360.732	512.313	–	–	15,436.522	14,924.209
TBX5	sgTv3-9	AGTGACAGGAGGGA GCAGTTTGG	–	–	–	–	–	381.584	418.221	–	–	399.903	18.318
TBX5	sgTv3-10	TGCTGGTAGCTGGA AACTGGGGG	–	–	–	–	–	6.473	22.619	–	–	14.546	8.073
TBX5	sgTv3-11	GCACCTCCGTTCCC AGCCGAAGG	–	–	–	–	–	3,237.790	2,387.540	–	–	2,812.665	425.125
TBX5	sgTv3-12	TAGTAACAGTAAT AATTCTAGGG	–	–	–	–	–	98.805	80.128	–	–	89.467	9.338
TBX5	sgTv3-13	AAAGTAATAGTAA TACTACTAGG	–	–	–	–	–	11.146	14.097	–	–	12.622	1.475
TBX5	sgTv3-14	ACCCGCGTCAGAC CCGGAGAAGG	–	–	–	–	–	49.323	50.656	–	–	49.990	0.666
TBX5	sgTv3-16	ATCACGGAGAGCC TGCGCAGGGG	–	–	–	–	–	6,474.837	6,722.309	–	–	6,598.573	123.736
TBX5	sgTv3-17	TATCACGGAGAGC CTGCGCAGGG	–	–	–	–	–	1,998.376	2,470.274	–	–	2,234.325	235.949
TBX5	sgTv3-18	TTATCACGGAGAG CCTGCGCAGG	–	–	–	–	–	651.057	946.434	–	–	798.745	147.688
TBX5	sgTv3-19	GACGGGCAGCTTG CTTATCACGG	–	–	–	–	–	2,752.702	3,050.598	–	–	2,901.650	148.948
TBX5	sgTv3-20	GAAGTCCAGACAA ATTTGACGGG	–	–	–	–	–	121.863	170.663	–	–	146.263	24.400
TBX5	sgTv3-21	AGAAGTCCAGACA AATTTGACGG	–	–	–	–	–	1.558	3.550	–	–	2.554	0.996
TBX5	sgTv3-26	ATTTTTGGAAGCC ACTGGGTAGG	–	–	–	–	–	691.631	780.797	–	–	736.214	44.583
TBX5	sgTv3-28	GAAATTCTCTAA AGGACACTGGG	–	–	–	–	–	14.393	13.128	–	–	13.761	0.633
TBX5	sgTv3-29	AGAAATTCTCTAA AGGACACTGG	–	–	–	–	–	4.952	3.883	–	–	4.417	0.535
TBX5	sgTv3-30	AGAAAACTATTCC TCTTGTGAGG	–	–	–	–	–	44.358	56.180	–	–	50.269	5.911
TBX5	sgTv4-1	GAGGTCTCTTGCA TAAGGCATGG	–	–	–	–	–	–	–	0.448	0.465	0.456	0.009
TBX5	sgTv4-2	AACCAGCTAGAGC GGCGCCTCGG	–	–	–	–	–	–	–	0.253	0.628	0.441	0.188
TBX5	sgTv4-3	CTTGGACCTTTCT CTCCGCAAGG	–	–	–	–	–	–	–	1.031	0.776	0.903	0.127

(*Continued on next page*)

Table 1. *Continued*

Gene	sgRNA ID	Target sequence	Experiment 1–replicate 1	Experiment 2–replicate 1	Experiment 2–replicate 2	Experiment 3–replicate 1	Experiment 3–replicate 2	Experiment 4–replicate 1	Experiment 4–replicate 2	Experiment 5–replicate 1	Experiment 5–replicate 2	Average vs. GAPDH	SEM
TBX5	sgTv4-4	AAATAGAGTGCCT CGTGCCTCGG	–	–	–	–	–	–	–	0.290	0.514	0.402	0.112
TBX5	sgTv4-5	GTTTTGCAACTCA ACCTAGTGGG	–	–	–	–	–	–	–	0.388	0.411	0.400	0.012
TBX5	sgTv4-6	AGAATCGAACCCC GAAGCTGGGG	–	–	–	–	–	–	–	0.564	0.234	0.399	0.165
TBX5	sgTv4-7	CATGCTTCGGAAA GCCCTGGGGG	–	–	–	–	–	–	–	2.066	1.102	1.584	0.482
TBX5	sgTv4-8	GAAGCTGCCCGCT CTCCCCGCGG	–	–	–	–	–	–	–	9.083	7.181	8.132	0.951
TBX5	sgTv4-9	TGGGAAACGAAAG CGAAGCTCGG	–	–	–	–	–	–	–	7.626	9.684	8.655	1.029
TBX5	sgTv4-10	AAACACGAGCCTC GGATTTGGGG	–	–	–	–	–	–	–	8.480	10.090	9.285	0.805

GAPDH, glyceraldehyde 3-phosphate dehydrogenase; NA, not applicable.

fibroblast-specific engineered nanoparticles would further accelerate the clinical translation of CRISPRa-based cardiac reprogramming.

After multiple rounds of empirical testing, we identified sgRNAs capable of activating endogenous MGT expression. However, optimizing our approaches to generate iCM with high molecular and functional fidelity, as well as robust efficiency, remains a significant challenge. Given the importance of *MEF2C* and *TBX5* in cardiac reprogramming, future work may focus on improving the endogenous activation of these factors. Notably, in both human and mouse fibroblasts, the most efficient M-sgRNAs tested were located tens of thousands of base pairs away from the TSS, highlighting the need for a more rational approach to target enhancer elements for the CRISPR strategy. To better understand how to improve reprogramming efficiency, a thorough comparison of the molecular and functional phenotypes of iCMs generated via endogenous activation or ectopic expression of MGT should be undertaken. These future studies will help elucidate the unique mechanism underlying CRISPRa-based cardiac reprogramming, advancing our understanding of the cell fate conversion process, as well as the epigenomic, transcriptomic, and proteomic remodeling involved.

MATERIALS AND METHODS

Mouse lines

Transgenic mice harboring GFP under the control of the αMHC promoter[9,10] were used for MEF and fCF preparation. Animal care was performed in accordance with the guidelines established by the University of North Carolina, Chapel Hill.

Generation of MEFs

Embryos from MHC-GFP reporter mice were harvested at embryonic days 12.5–14.5, and their internal organs and head were removed as previously described.[16] The body below the head was minced to small pieces and incubated at 37°C for 15 min in 1 mL 0.05% trypsin-EDTA with 100 Kunitz units of DNase I per embryo. After centrifuging, the supernatant was carefully removed and the cell pellet was resuspended in warm MEF medium (DMEM/10% fetal bovine serum [FBS], 50 U/50 μg/mL penicillin/streptomycin, and 1% GlutaMAX supplement [Gibco]) and then plated on a 10-cm dish. The MEF media was changed 24 h after plating. Cells are generally 80%–90% confluent 24 h after plating. MEFs were harvested at 72 h and stored for future use.

Generation of neonatal CFs

Hearts were removed from αMHC-GFP transgenic mice and rinsed thoroughly with chilled PBS to remove blood and other tissues. The hearts were then minced roughly into 1 × 1 mm pieces, transferred to a 50-mL conical tube with 20 mL warm 0.05% trypsin-EDTA, and incubated at 37°C for 20 min. The supernatant was discarded, and the heart pieces were digested with 10 mL warm 0.2% collagenase type II in Hank's balanced salt solution for 7 min at 37°C, followed by vortexing for 1 min. The supernatant was collected and diluted with 7 mL fibroblast medium. After five rounds of collagenase digestion and collection, a single-cell suspension was obtained by passing the

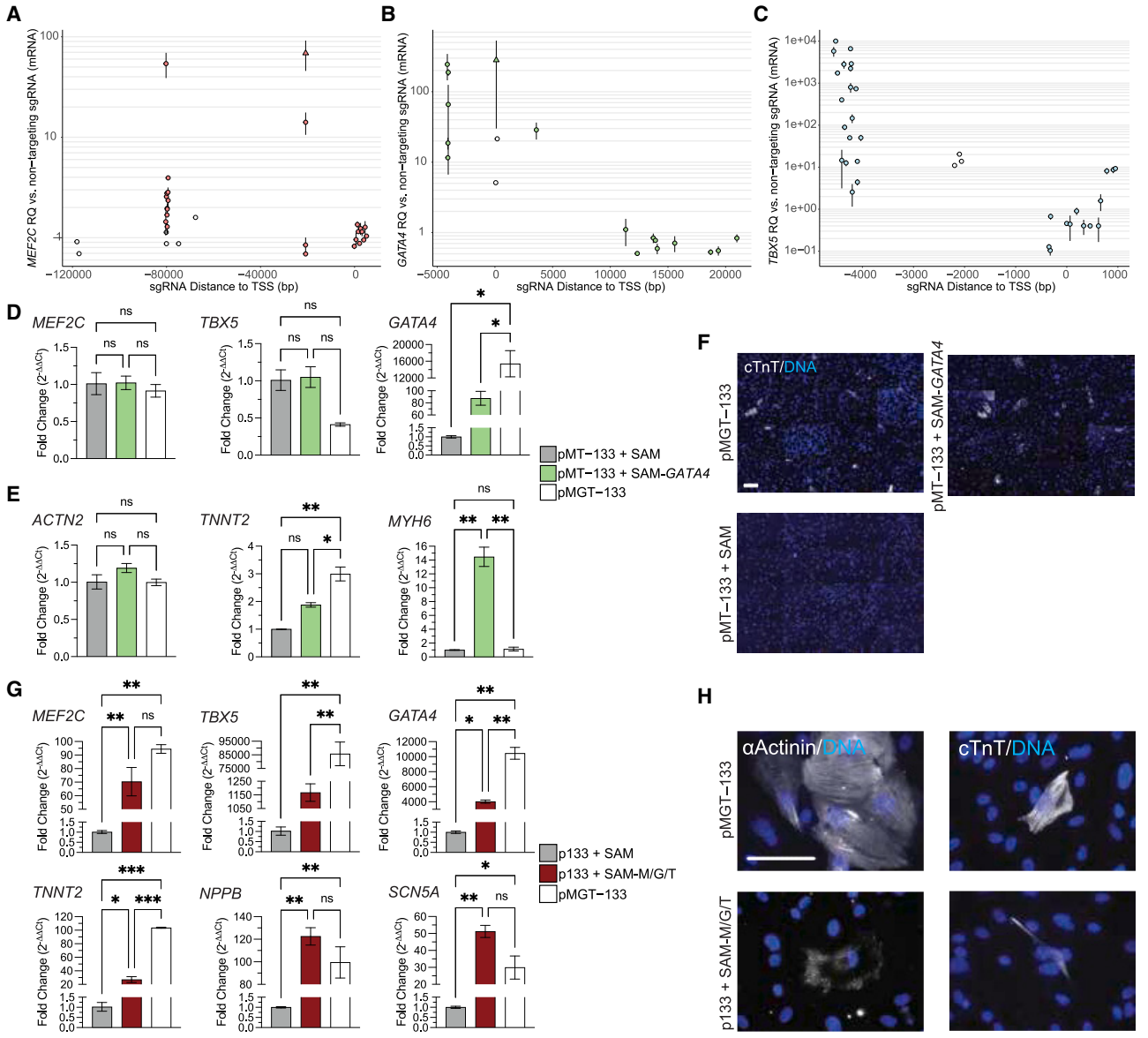

Figure 6. Reprogramming H9Fs into iCMs via CRISPRa-mediated activation of *GATA4*, *MEF2C*, and *TBX5*

(A–C) Summary of sgRNAs tested for CRISPRa-mediated activation of *MEF2C* (A), *GATA4* (B), and *TBX5* (C). Data represent six independent experiments. Point range plots illustrate the activation levels induced by each sgRNA and their relative position to the TSS. Open circles, one replicate; filled circles, two replicates, one experiment; filled triangles, three or more replicates, two or more experiments. (D–F) Replacement of retroviral overexpressing *GATA4* with SAM-*GATA4*. (D) qPCR analysis at day 2. The y axis indicates fold change by $2^{-\Delta\Delta Ct}$ relative to control pMT−133+SAM. $n = 2$ biological replicates. (E) qPCR analysis at day 10. The y axis indicates fold change by $2^{-\Delta\Delta Ct}$ relative to the pMT−133+SAM control. $n = 2$ biological replicates. (F) Tiled composite images of ICC staining for cTnT at day 14, with 40× images captured from 16 random fields per well. (G and H) CRISPRa activation of all three reprogramming factors with SAM-MGT (G) qPCR at day 14. The y axis indicates fold change by $2^{-\Delta\Delta Ct}$ relative to the pMT−133+SAM control. $n = 2$ biological replicates. (H) Representative images of ICC staining for sarcomere components at day 14, acquired at 40× magnification. ns, not significant. Scale bars, 100 μm $^{*}p < 0.05$; $^{**}p < 0.01$.

cell solution through a 40-μm cell strainer. The cell suspension was then neutralized with fibroblast media. After centrifuging, the cell pellet was resuspended in 1 mL Red cell lysis buffer (150 mM NH_4Cl, 10 mM $KHCO_3$, and 0.1 mM EDTA) for 1 min on ice and then resuspended in MACS buffer (Dulbecco's PBS with 0.5% BSA and 2 mM EDTA) for cell sorting.

H9F derivation and culture

Fibroblasts were previously differentiated from H9 embryonic stem cells and subcultured.[34] Cells were expanded, frozen, and stored in liquid nitrogen. A new vial of cells was thawed for each experiment performed, and the cells were passaged at least once prior to seeding for infection. H9Fs were maintained in DMEM 20% FBS 1×

non-essential amino acid medium (NEAA) 1× penicillin/streptomycin and kept in an aseptic incubator at 37°C 5% CO_2 90% relative humidity.

Magnetic cell sorting

Thy1.2$^+$ CFs were isolated by magnetic-activated cell sorting (MACS; Miltenyi Biotec) according to the manufacturer's instructions. Briefly, cells (about 1×10^7) were suspended in 90 μL MACS buffer and incubated with 10 μL Thy1.2 biotin anti-mouse CD90.2 antibody (eBioscience, Invitrogen) for 30 min at 4°C. The cell/Thy1.2 biotin anti-mouse CD90.2 antibody/MACS solution was resuspended in 5 mL MACS buffer and centrifuged at 300 × *g* for 5 min. The supernatant was discarded. The cell/Thy1.2 biotin anti-mouse CD90.2 antibody pellet was then suspended in 90 μL MACS buffer and incubated with 10 μL Anti-Biotin MicroBeads (Miltenyi Biotec) at 4°C for 30 min. The cell/Thy1.2 biotin anti-mouse CD90.2 antibody/Anti-Biotin MicroBeads solution was resuspended in MACS buffer, passed through a 30-μm nylon mesh, and applied to an MACS calibrated LS column. Target cells were flushed out after with two MACS washes and resuspended in explant culture medium for further usage.

Plasmids

Retroviral vectors encoding mouse and human GMT and polycistronic MGT in pMXs-based vectors were described previously.[9,10,38,39] To generate the lentiviral vectors encoding GMT targeted sgRNAs, a DNA fragment containing oligonucleotides encoding sgRNAs was synthesized and cloned into SAMv2 vector (Addgene 75112). Lentiviral vector encoding the MS2-P65-HSF1 activator helper complex lentiMPHv2 was also purchased from Addgene (89308).

Cell culture, transfections, and viral transductions

Fibroblasts were maintained in normal or high serum media during viral transduction and subsequently cultured in iCM medium (10% FBS and 90% DMEM/M199 [4:1]) for the duration of the experiment to promote cardiac reprogramming and maturation. PlatE packaging cells (for retrovirus production) and HEK293T cells (for lentivirus production) were maintained in growth media containing DMEM plus 10% FBS, 50 U/50 μg/mL penicillin/streptomycin, 1 μg/mL puromycin (Sigma), and 100 μg/mL of blasticidin S (Life Technologies). All transfections were performed using Lipofectamine 2000 (Invitrogen) in accordance with the manufacturer's protocol. For positive selection, puromycin (for retrovirus) or blasticidin S and hygromycin (for CRISPRa lentiviruses) were added to transformed cells 3 days after infection. For MEF, fCF, and H9F, concentrations of 2 μg/mL puromycin and 150 μg/mL hygromycin were used for positive selection. For MEF and fCF, a concentration of 100 μg/mL of blasticidin S was used for positive selection, while a concentration of 15 μg/mL blasticidin S was used for positive selection in H9F.

Real-time qPCR

RNA was extracted with Trizol (Invitrogen). First strand cDNAs were synthesized using the Superscript IV first-strand synthesis system (Invitrogen). qRT-PCR with SYBR Green Master Mix was performed using a QuantStudio 6 real-time qPCR system (Applied Biosystems) per the manufacturer's protocols.

Flow cytometry

At 10 days' post-infection, the reprogrammed cells were washed with PBS and dissociated with 0.05% trypsin (Life Technologies) for 5 min at 37°C. Cells were washed twice with pre-cold fluorescence-activated cell sorting (FACS) buffer (Dulbecco's PBS supplemented with 2% FBS and 2 mM EDTA) and subjected to fixation and staining with cell fixation/permeabilization kits (BD Biosciences). Cells were incubated with antibodies at 4°C for 30 min at concentrations recommended by manufacturers. Cells were then suspended with staining buffer (Dulbecco's PBS with 1% paraformaldehyde) and counted using the BD Accuri C6 flow cytometer. FACS data were analyzed by FlowJo software (Tree Star). The following antibodies were used: mouse anti-troponin T, cardiac isoform (Thermo Scientific, 1:400), rabbit anti-GFP immunoglobulin G (IgG; Invitrogen, 1:500), rabbit anti-α-actinin, (Abcam, ab68167, 1:500), Alexa Fluor 488-conjugated donkey anti-rabbit IgG, and Alexa Fluor 647-conjugated donkey anti-mouse IgG (Jackson ImmunoResearch, 1:500).

Immunofluorescence staining

Cells were washed three times with ice-cold PBS and fixed with 4% paraformaldehyde (EMS) at room temperature (RT) for 15 min. For staining, cells were permeabilized with 0.1% Triton/PBS for 30 min and blocked with 5% BSA for 1 h prior to primary antibody incubation at 4°C overnight. Following primary antibody incubation, cells were washed with PBS three times and then secondary antibody was applied for 1 h at RT. Nuclear staining was performed with DAPI in mounting medium Vectashield (Vector Labs). The following primary antibodies were used: cTnT (Thermo Scientific, 1:400), GFP (Invitrogen, 1:500), and α-actinin, (Abcam, ab68167, 1:500). Images were acquired using the EVOS FL Auto Cell Imaging System (Life Technologies).

Western blot

Cells were collected and lysed in 2× SDS loading buffer (Bio-Rad) and subjected to SDS-PAGE. After separation, proteins were transferred to nitrocellulose membranes and probed with the indicated antibodies. The target proteins were detected by chemiluminescence (ECL, Thermo Scientific). The membranes were stripped with stripping buffer (Sigma) and re-probed with antibody against a second protein or β-actin for loading control.

Statistical methods

Statistical analysis was done using GraphPad Prism 8. All data were analyzed with at least three biological replicates and presented as mean ± SEM. Differences between groups were examined for statistical significance using two-way unpaired Student's t test, a one-way ANOVA, or a two-way ANOVA. A $p < 0.05$ was regarded as significant.

DATA AND CODE AVAILABILITY

All the data related to this study are available within the paper or can be obtained from the authors on request.

ACKNOWLEDGMENTS

We thank all the members of the Qian laboratory for helpful discussions and valuable input. This work was supported by American Heart Association (AHA) grant 20EIA35310348 and NIH National Heart, Lung, and Blood Institute (NHLBI) grant R35HL155656 to L.Q. and NIH NHLBI grants R01HL139976 and R01HL139880 and AHA Established Investigator Award 20EIA35320128 to J.L.

AUTHOR CONTRIBUTIONS

P.H. and J.X. conceived the project, performed the experiments, and wrote the manuscript, with contributions from all other authors. Y. Xie, B.K., D.N., Y. Xu, and J.R.H. assisted with experiments and data analysis. S.R. and B.S. assisted with data analysis and edited the manuscript. J.L. edited the manuscript. L.W. and L.Q. supervised the project, provided the funding, and edited the manuscript.

DECLARATION OF INTERESTS

The authors declare no competing interests.

SUPPLEMENTAL INFORMATION

Supplemental information can be found online at https://doi.org/10.1016/j.omtn.2024.102390.

REFERENCES

1. Benjamin, E.J., Muntner, P., Alonso, A., Bittencourt, M.S., Callaway, C.W., Carson, A.P., Chamberlain, A.M., Chang, A.R., Cheng, S., Das, S.R., et al. (2019). Heart disease and stroke statistics—2019 update: A report from the american heart association. Circulation *139*, e56–e528.
2. Laflamme, M.A., and Murry, C.E. (2011). Heart regeneration. Nature *473*, 326–335.
3. Doenst, T., Haverich, A., Serruys, P., Bonow, R.O., Kappetein, P., Falk, V., Velazquez, E., Diegeler, A., and Sigusch, H. (2019). Pci and cabg for treating stable coronary artery disease: Jacc review topic of the week. J. Am. Coll. Cardiol. *73*, 964–976.
4. Bergmann, O., Zdunek, S., Felker, A., Salehpour, M., Alkass, K., Bernard, S., Sjostrom, S.L., Szewczykowska, M., Jackowska, T., Dos Remedios, C., et al. (2015). Dynamics of cell generation and turnover in the human heart. Cell *161*, 1566–1575.
5. Kimura, W., Xiao, F., Canseco, D.C., Muralidhar, S., Thet, S., Zhang, H.M., Abderrahman, Y., Chen, R., Garcia, J.A., Shelton, J.M., et al. (2015). Hypoxia fate mapping identifies cycling cardiomyocytes in the adult heart. Nature *523*, 226–230.
6. Nakada, Y., Canseco, D.C., Thet, S., Abdisalaam, S., Asaithamby, A., Santos, C.X., Shah, A.M., Zhang, H., Faber, J.E., Kinter, M.T., et al. (2017). Hypoxia induces heart regeneration in adult mice. Nature *541*, 222–227.
7. Senyo, S.E., Steinhauser, M.L., Pizzimenti, C.L., Yang, V.K., Cai, L., Wang, M., Wu, T.D., Guerquin-Kern, J.L., Lechene, C.P., and Lee, R.T. (2013). Mammalian heart renewal by pre-existing cardiomyocytes. Nature *493*, 433–436.
8. Xu, J., Du, Y., and Deng, H. (2015). Direct lineage reprogramming: strategies, mechanisms, and applications. Cell Stem Cell *16*, 119–134.
9. Ieda, M., Fu, J.D., Delgado-Olguin, P., Vedantham, V., Hayashi, Y., Bruneau, B.G., and Srivastava, D. (2010). Direct reprogramming of fibroblasts into functional cardiomyocytes by defined factors. Cell *142*, 375–386.
10. Qian, L., Huang, Y., Spencer, C.I., Foley, A., Vedantham, V., Liu, L., Conway, S.J., Fu, J.D., and Srivastava, D. (2012). In vivo reprogramming of murine cardiac fibroblasts into induced cardiomyocytes. Nature *485*, 593–598.
11. Song, K., Nam, Y.J., Luo, X., Qi, X., Tan, W., Huang, G.N., Acharya, A., Smith, C.L., Tallquist, M.D., Neilson, E.G., et al. (2012). Heart repair by reprogramming non-myocytes with cardiac transcription factors. Nature *485*, 599–604.
12. Wang, H., Cao, N., Spencer, C.I., Nie, B., Ma, T., Xu, T., Zhang, Y., Wang, X., Srivastava, D., and Ding, S. (2014). Small molecules enable cardiac reprogramming of mouse fibroblasts with a single factor, Oct4. Cell Rep. *6*, 951–960.
13. Chavez, A., Scheiman, J., Vora, S., Pruitt, B.W., Tuttle, M., P R Iyer, E., Lin, S., Kiani, S., Guzman, C.D., Wiegand, D.J., et al. (2015). Highly efficient Cas9-mediated transcriptional programming. Nat. Methods *12*, 326–328.
14. Perez-Pinera, P., Kocak, D.D., Vockley, C.M., Adler, A.F., Kabadi, A.M., Polstein, L.R., Thakore, P.I., Glass, K.A., Ousterout, D.G., Leong, K.W., et al. (2013). RNA-guided gene activation by CRISPR-Cas9-based transcription factors. Nat. Methods *10*, 973–976.
15. Chavez, A., Tuttle, M., Pruitt, B.W., Ewen-Campen, B., Chari, R., Ter-Ovanesyan, D., Haque, S.J., Cecchi, R.J., Kowal, E.J.K., Buchthal, J., et al. (2016). Comparison of Cas9 activators in multiple species. Nat. Methods *13*, 563–567.
16. Konermann, S., Brigham, M.D., Trevino, A.E., Joung, J., Abudayyeh, O.O., Barcena, C., Hsu, P.D., Habib, N., Gootenberg, J.S., Nishimasu, H., et al. (2015). Genome-scale transcriptional activation by an engineered CRISPR-Cas9 complex. Nature *517*, 583–588.
17. Dodou, E., Xu, S.M., and Black, B.L. (2003). mef2c is activated directly by myogenic basic helix-loop-helix proteins during skeletal muscle development *in vivo*. Mech. Dev. *120*, 1021–1032.
18. Dodou, E., Verzi, M.P., Anderson, J.P., Xu, S.M., and Black, B.L. (2004). Mef2c is a direct transcriptional target of ISL1 and GATA factors in the anterior heart field during mouse embryonic development. Development *131*, 3931–3942.
19. De Val, S., Anderson, J.P., Heidt, A.B., Khiem, D., Xu, S.M., and Black, B.L. (2004). Mef2c is activated directly by Ets transcription factors through an evolutionarily conserved endothelial cell-specific enhancer. Dev. Biol. *275*, 424–434.
20. Lin, B.R., and Natarajan, V. (2012). Negative regulation of human U6 snRNA promoter by p38 kinase through Oct-1. Gene *497*, 200–207.
21. Zhou, Y., Zhu, S., Cai, C., Yuan, P., Li, C., Huang, Y., and Wei, W. (2014). High-throughput screening of a CRISPR/Cas9 library for functional genomics in human cells. Nature *509*, 487–491.
22. GTEx Consortium (2013). The Genotype-Tissue Expression (GTEx) project. Nat. Genet. *45*, 580–585.
23. Visel, A., Minovitsky, S., Dubchak, I., and Pennacchio, L.A. (2007). VISTA Enhancer Browser–a database of tissue-specific human enhancers. Nucleic Acids Res. *35*, D88–D92.
24. ENCODE Project Consortium (2012). An integrated encyclopedia of DNA elements in the human genome. Nature *489*, 57–74.
25. Xu, H., Xiao, T., Chen, C.H., Li, W., Meyer, C.A., Wu, Q., Wu, D., Cong, L., Zhang, F., Liu, J.S., et al. (2015). Sequence determinants of improved CRISPR sgRNA design. Genome Res. *25*, 1147–1157.
26. Zhou, Y., Liu, Z., Welch, J.D., Gao, X., Wang, L., Garbutt, T., Keepers, B., Ma, H., Prins, J.F., Shen, W., et al. (2019). Single-Cell Transcriptomic Analyses of Cell Fate Transitions during Human Cardiac Reprogramming. Cell Stem Cell *25*, 149–164.e9.
27. Muraoka, N., Yamakawa, H., Miyamoto, K., Sadahiro, T., Umei, T., Isomi, M., Nakashima, H., Akiyama, M., Wada, R., Inagawa, K., et al. (2014). MiR-133 promotes cardiac reprogramming by directly repressing Snai1 and silencing fibroblast signatures. EMBO J. *33*, 1565–1581.
28. Black, J.B., Adler, A.F., Wang, H.G., D'Ippolito, A.M., Hutchinson, H.A., Reddy, T.E., Pitt, G.S., Leong, K.W., and Gersbach, C.A. (2016). Targeted Epigenetic Remodeling of Endogenous Loci by CRISPR/Cas9-Based Transcriptional Activators Directly Converts Fibroblasts to Neuronal Cells. Cell Stem Cell *19*, 406–414.
29. Clark, T., Waller, M.A., Loo, L., Moreno, C.L., Denes, C.E., and Neely, G.G. (2024). CRISPR activation screens: navigating technologies and applications. Trends Biotechnol. *42*, 1017–1034.
30. Chen, G.H., Xu, J., and Yang, Y.J. (2017). Exosomes: promising sacks for treating ischemic heart disease? Am J Physiol *Heart Circ Physiol*. Am. J. Physiol. Heart Circ. Physiol. *313*, H508–H523.
31. Afzal, M.R., Samanta, A., Shah, Z.I., Jeevanantham, V., Abdel-Latif, A., Zuba-Surma, E.K., and Dawn, B. (2015). Adult Bone Marrow Cell Therapy for Ischemic Heart Disease: Evidence and Insights From Randomized Controlled Trials. Circ. Res. *117*, 558–575.
32. Srivastava, D., and DeWitt, N. (2016). In Vivo Cellular Reprogramming: The Next Generation. Cell *166*, 1386–1396.
33. Mathison, M., Singh, V.P., Chiuchiolo, M.J., Sanagasetti, D., Mao, Y., Patel, V.B., Yang, J., Kaminsky, S.M., Crystal, R.G., and Rosengart, T.K. (2017). In situ

reprogramming to transdifferentiate fibroblasts into cardiomyocytes using adenoviral vectors: Implications for clinical myocardial regeneration. J. Thorac. Cardiovasc. Surg. *153*, 329–339.e3.

34. Jayawardena, T.M., Finch, E.A., Zhang, L., Zhang, H., Hodgkinson, C.P., Pratt, R.E., Rosenberg, P.B., Mirotsou, M., and Dzau, V.J. (2015). MicroRNA induced cardiac reprogramming *in vivo*: evidence for mature cardiac myocytes and improved cardiac function. Circ. Res. *116*, 418–424.

35. Jayawardena, T.M., Egemnazarov, B., Finch, E.A., Zhang, L., Payne, J.A., Pandya, K., Zhang, Z., Rosenberg, P., Mirotsou, M., and Dzau, V.J. (2012). MicroRNA-mediated *in vitro* and *in vivo* direct reprogramming of cardiac fibroblasts to cardiomyocytes. Circ. Res. *110*, 1465–1473.

36. Jayawardena, T., Mirotsou, M., and Dzau, V.J. (2014). Direct reprogramming of cardiac fibroblasts to cardiomyocytes using microRNAs. Methods Mol. Biol. *1150*, 263–272.

37. Fu, Y., Huang, C., Xu, X., Gu, H., Ye, Y., Jiang, C., Qiu, Z., and Xie, X. (2015). Direct reprogramming of mouse fibroblasts into cardiomyocytes with chemical cocktails. Cell Res. *25*, 1013–1024.

38. Wang, L., Liu, Z., Yin, C., Asfour, H., Chen, O., Li, Y., Bursac, N., Liu, J., and Qian, L. (2015). Stoichiometry of Gata4, Mef2c, and Tbx5 influences the efficiency and quality of induced cardiac myocyte reprogramming. Circ. Res. *116*, 237–244.

39. Wang, L., Huang, P., Near, D., Ravi, K., Xu, Y., Liu, J., and Qian, L. (2020). Isoform specific effects of Mef2C during direct cardiac reprogramming. Cells *9*, 268.